Maslen C, Babcock D, Raghunath M, Steinmann B. 1997. A rare branch-point mutation is associated with missplicing of fibrillin-2 in a large family with congenital contractural arachnodactyly. Am J Hum Genet 60:1389–1398.

Matyas G, Arnold E, Carrel T, Baumgartner D, Boileau C, Berger W, Steinmann B. 2006. Identification and in silico analyses of novel TGFBR1 and TGFBR2 mutations in Marfan syndrome-related disorders. Hum Mutat 27:760–769.

Mizuguchi T, Collod-Beroud G, Akiyama T, Abifadel M, Harada N, Morisaki T, Allard D, Varret M, Claustres M, Morisaki H, Ihara M, Kinoshita A, Yoshiura K, Junien C, Kajii T, Jondeau G, Ohta T, Kishino T, Furukawa Y, Nakamura Y, Niikawa N, Boileau C, Matsumoto N. 2004. Heterozygous TGFBR2 mutations in Marfan syndrome. Nat Genet 36 :855–860.

Pannu H, Fadulu VT, Chang J, Lafont A, Hasham SN, Sparks E, Giampietro PF, Zaleski C, Estrera AL, Safi HJ, Shete S, Willing MC, Raman CS, Milewicz DM. 2005. Mutations in transforming growth factor-beta receptor type II cause familial thoracic aortic aneurysms and dissections. Circulation 112:513–520.

Park ES, Putnam EA, Chitayat D, Child A, Milewicz DM. 1998. Clustering of FBN2 mutations in patients with congenital contractural arachnodactyly indicates an important role of the domains encoded by exons 24 through 34 during human development. Am J Med Genet 78:350–355.

Pereira L, Andrikopoulos K, Tian J, Lee SY, Keene DR, Ono R, Reinhardt DP, Sakai LY, Biery NJ, Bunton T, Dietz HC, Ramirez F. 1997. Targeting of the gene encoding fibrillin-1 recapitulates the vascular aspect of Marfan syndrome. Nat Genet 17:218–222.

Pereira L, Lee SY, Gayraud B, Andrikopoulos K, Shapiro SD, Bunton T, Biery NJ, Dietz HC, Sakai LY, Ramirez F. 1999. Pathogenetic sequence for aneurysm revealed in mice underexpressing fibrillin-1. Proc Natl Acad Sci USA 96:3819–3823.

Putnam EA, Zhang H, Ramirez F, Milewicz DM. 1995. Fibrillin-2 (FBN2) mutations result in the Marfan-like disorder, congenital contractural arachnodactyly. Nat Genet 11:456–458.

Putnam EA, Park ES, Aalfs CM, Hennekam RC, Milewicz DM. 1997. Parental somatic and germ-line mosaicism for a FBN2 mutation and analysis of FBN2 transcript levels in dermal fibroblasts. Am J Hum Genet 60:818–827.

Pyeritz RE. 2000. The Marfan syndrome. Annu Rev Med 51:481–510.

Sakai H, Visser R, Ikegawa S, Ito E, Numabe H, Watanabe Y, Mikami H, Kondoh T, Kitoh H, Sugiyama R, Okamoto N, Ogata T, Fodde R, Mizuno S, Takamura K, Egashira M, Sasaki N, Watanabe S, Nishimaki S, Takada F, Nagai T, Okada Y, Aoka Y, Yasuda K, Iwasa M, Kogaki S, Harada N, Mizuguchi T, Matsumoto N. 2006. Comprehensive genetic analysis of relevant four genes in 49 patients with Marfan syndrome or Marfan-related phenotypes. Am J Med Genet Part A 140A: 1719–1725.

Singh KK, Rommel K, Mishra A, Karck M, Haverich A, Schmidtke J, Arslan-Kirchner M. 2006. TGFBR1 and TGFBR2 mutations in patients with features of Marfan syndrome and Loeys-Dietz syndrome. Hum Mutat 27:770–777.

Tiecke F, Katzke S, Booms P, Robinson PN, Neumann L, Godfrey M, Mathews KR, Scheuner M, Hinkel GK, Brenner RE, Hovels-Gurich HH, Hagemeier C, Fuchs J, Skovby F, Rosenberg T. 2001. Classic, atypically severe and neonatal Marfan syndrome: Twelve mutations and genotype-phenotype correlations in FBN1 exons 24–40. Eur J Hum Genet 9:13–21.

Viljoen D. 1994. Congenital contractural arachnodactyly (Beals syndrome). J Med Genet 31:640–643.

Wang M, Clericuzio CL, Godfrey M. 1996. Familial occurrence of typical and severe lethal congenital contractural arachnodactyly caused by missplicing of exon 34 of fibrillin-2. Am J Hum Genet 59:1027–1034.

Acta Med. Nagasaki 52: 29—34

Less Frequent *NSD1*-Intragenic Deletions in Japanese Sotos Syndrome: Analysis of 30 Patients by *NSD1*-Exon Array CGH, Quantitative Fluorescent Duplex PCR, and Fluorescence In Situ Hybridization

Nadiya SOSONKINA,[1,2,3] Noriko MIYAKE,[2] Naoki HARADA,[3,4] Dmytro STARENKI,[1,3] Tohru OHTA,[1,3] Yoshimitsu FUKUSHIMA,[5] Tomoki KOSHO,[5] Norio NIIKAWA,[2,3] Naomichi MATSUMOTO[3,6]

[1]The Research Institute of Personalized Health Sciences, Health Sciences University of Hokkaido, Sapporo, Japan
[2]Department of Human Genetics, Nagasaki University Graduate School of Biomedical Sciences, Nagasaki, Japan
[3]SORST, Japan Science and Technology Agency, Kawaguchi, Japan
[4]Kyushu Medical Science Nagasaki Laboratory, Nagasaki, Japan
[5]Department of Medical Genetics, Shinshu University School of Medicine, Matsumoto, Japan
[6]Department of Human Genetics, Yokohama City University Graduate School of Medicine, Yokohama, Japan

Sotos syndrome (SoS, OMIM #117550) is an autosomal dominant overgrowth syndrome with pre- and postnatal excessive growth, characteristic craniofacial features, and variable degrees of developmental delay. Haploinsufficiency of the nuclear receptor binding SET domain containing protein 1 (*NSD1*) gene causes SoS, as two thirds of SoS patients had either a whole-gene microdeletion or an intragenic point mutation. However, the etiology of other patients remains undetermined. In the present study, we analyzed 30 Japanese SoS patients on whether they have *NSD1* intragenic deletions by *NSD1*-specific exon microarray comparative genomic hybridization (array CGH). Although the analysis suggested a deletion at the 5' region of *NSD1* in 16 of the 30 patients, no such abnormalities were confirmed by subsequent quantitative fluorescent duplex PCR and fluorescence *in situ* hybridization. As no intragenic deletions have been identified in our series of SoS patients, other genetic aberrations need to be identified.

ACTA MEDICA NAGASAKIENSIA 52: 29—34, 2007

Keywords: Sotos syndrome; *NSD1*; Intragenic deletion; Exon array CGH; Quantitative fluorescent duplex PCR

Introduction

Sotos syndrome (SoS, OMIM #117550) is an overgrowth disorder characterized by excessive growth in childhood, distinctive craniofacial features, including macrocephaly, and mental retardation. SoS is caused by haploinsufficiency of the nuclear receptor binding SET domain containing protein 1 gene (*NSD1*) located at 5q35.2-q35.3.[1] Microdeletions encompassing the entire *NSD1* and intragenic point mutations account for about 50% and 10% of Japanese patients, respectively.[1-3] On the other hand, the point mutations are the main disease-causing abnormalities in non-Japanese patients (50% or more), and microdeletions occur in about 10% of them.[4-10] The reason for the difference between Japanese and non-Japanese patient groups remains unexplained. Partial, intragenic deletions of *NSD1*, comprising a single or multiple exons, were recently found by multiplex ligation-dependent probe amplification (MLPA) method in eight (6 %) of 124 SoS patients from UK.[11] As the etiology of about one third of Japanese SoS patients is undetermined, we hypothesized that intragenic deletions could frequently be associated with Japanese SoS patients. For analysis of such deletions, we developed an *NSD1*-specific exon microarray comparative genome hybridization (array CGH) system.

Here we report the results of analysis of 30 Japanese patients with SoS.

Materials and Methods

Subjects

The research was approved by the Committee for Ethical Issues

Address correspondence: Naomichi Matsumoto, M.D., Ph.D., Department of Human Genetics, Yokohama City University Graduate School of Medicine, Fukuura 3-9, Kanazawa-ku, Yokohama 236-0004 JAPAN
TEL : +81-(0)45-787-2606, FAX : +81-(0)45-786-5219, E-mail: naomat@yokohama-cu.ac.jp

Received December 5, 2006 ; Accepted February 23, 2007

on Human Genome and Gene Analysis at Nagasaki University. The subjects studied included 30 patients (seven females and 23 males) with typical SoS features (including macrocephaly, overgrowth, and mental retardation), in whom a whole-*NSD1* gene microdeletion and *NSD1* point mutation were excluded. Clinical manifestations of these cases were reported elsewhere.[2,3] After obtaining informed consent, DNA was isolated from patients' peripheral blood leukocytes. We also used DNA samples from six other patients with SoS who had been previously diagnosed to have a whole-gene deletion, as positive controls in microarray conperative genomic hybridization (CGH) and quantitative fluorescent duplex PCR experiments.

NSD1-specific exon array CGH

A total of 34 genomic regions were selected from the *NSD1* locus, chromosome X, and from chromosome 13 as elements for *NSD1*-specific exon array CGH: Five from an 18-kb segment upstream of *NSD1*, 23 exons of *NSD1*, and three regions from each of chromosomes X and 13 (Figure 2). Sequences of all these regions are unique according to RepeatMasker program (http://www.repeatmasker.org/), and range from 355 bp to 2765 bp (primer sequences and conditions for elements amplification available on request). PCR products of the regions were cloned into pCR™2.1-TOPO™ vector (Invitrogen, Carlsbad, CA), and used for transformation of DH5α-T1™ (Invitrogen). Insert sequences were confirmed on ABI Genetic Analyzer 3100 (Applied Biosystems, Foster City, CA), and they were then amplified from corresponding plasmids using universal 5'-amino-linked primers (forward: TACCGAGCTCGGATCCACTAGTA; reverse: CAGTGTGATGGATATCTGDCA) by PCR in a volume of 100 μL. PCR products were purified with a membrane filter, Microcon YM-30 (Millipore, Badford, MA), dissolved in 0.25 M phosphate buffer/0.00025% N-lauroyl sacrosine, and spotted in quadruplicate on CodeLink™ aminosilane coated slides (Amersham Bioscience, Piscataway, NJ) with a single pin spotter, Stampman (Nippon Laser and Electronics Laboratory, Nagoya, Japan). The same set of probes was printed twice on one glass slide, forming Block-1 and Block-2. The slides were finally treated as described previously,[12] and stored at room temperature and low humidity until use.

After complete digestion with *Eco*RI, subject DNA (800 ng) was labeled with Cy-3 dCTP (GE Healthcare Bio-Sciences, Piscataway, NJ) and the same amount of reference DNA (with an opposite sex) was labeled with Cy-5 dCTP using Bioprime DNA Labeling Kit (Invitrogen) (Block-1). Dyes were swapped in Block-2 (subject DNA labeled with Cy5 and reference DNA labeled with Cy3) to confirm that signal patterns were opposite. Prehybridization and hybridization procedures were carried out as described previously.[13] Processed arrays were scanned with GenePix 4000B (Axon Instruments, Union City, CA) and analyzed with GenePix Pro 4.0 software (Axon Instruments). Signal intensity ratios between subject and reference DNA were calculated from the data of the single-slide experiment, using the ratio of means formula according to GenePix Pro. 4.0:

$$\text{Ratio Cy5/Cy3} = \frac{\text{mean Cy5 intensity of feature-median Cy5 intensity of the background}}{\text{mean Cy3 intensity of feature-median Cy3 intensity of the background}}$$

Ratios of all array elements were normalized to the average of elements from chromosome 13 as an internal normal control. The signal ratio was regarded as "abnormal," when it was out of ±3 SD (standard deviation) range which was determined from three elements of chromosome 13.

Quantitative fluorescent duplex PCR (QFD-PCR)

With a QFD-PCR method described previously,[14,15] we designed test primers to amplify a 302-bp region "A" that is corresponding to the 5'-5 region (Figure 1). Reverse primer was labeled at its 5' end

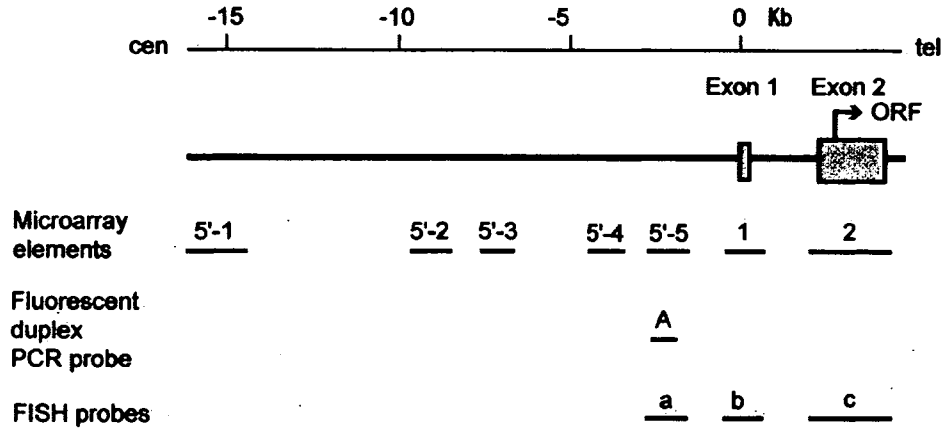

Figure 1. Schematic representation of a 20-kb segment covered by microarray. Exons 1 and 2 of the *NSD1* gene are presented as grey boxes, open reading frame (ORF) of *NSD1* starts from an arrow. Seven elements of the exon array are shown: five (5'-1, 5'-2, 5'-3, 5'-4, and 5'-5) covering the *NSD1* upstream region; two (1, 2) covering exons 1 and 2, and adjacent areas. Region A is a probe for QFD-PCR, and a, b and c are probes for FISH analysis.

with 6-FAM fluorophore (Applied Biosystems). Non-polymorphic STS marker G06854 (330 bp) mapped at 10q25.3 was chosen as an internal control, and control primers were designed according UCSC Genome Bioinformatics web site (http://genome.ucsc.edu). Reverse primer was labeled at its 5' end with HEX fluorophore (Applied Biosystems). Test and control regions were amplified simultaneously in a single tube. Reaction was carried out in a volume of 20 μL, containing 100 ng of template DNA, 1 X ExTaq buffer, 200 μM of each dNTP, 1 U of ExTaq DNA polymerase (Takara, Otsu, Japan), and 0.2 μM of test primers (forward: GTTGAGTCGAATT GCCCAGAT; reverse: ACAGGCCCTTAGCACATGTCT), and 0.3 μM of control primers (forward: AGACAGGGTTGGGAAGG ACT; reverse: CAGGAGAGCCTTGGTGAAAG). After an initial step of denaturation at 95 °C for 3 min, PCR was cycled 27 times at 95 °C for 30 sec, at 62 °C for 30 sec, and at 72 °C for 25 sec, followed by the final extension at 72 °C for 4 min. An aliquot (2 μL) of PCR products was mixed with 16 μL formamide, and the mixture (2 μL) was further combined with 2.5 μL loading buffer containing 0.3 μL of GENESCAN™-500XL size standard (Applied Biosystems). Samples were separated with ABI 377 automated sequencer (Applied Biosystems), and results were analyzed using GeneScan 3.1.2 and Genotyper 2.5 (Applied Biosystems).

We analyzed all but two SoS patients (SoS 151 and SoS 149) whose DNA was used up, six patients confirmed to have a 5q35 whole-gene deletion as positive controls, and six normal controls. To determine an *NSD1* intragenic deletion, we adopted a method described by Yau et al.,[15] and calculated 6 dosage quotients (DQ) for each SoS patient to be examined and each positive control patient using peak heights, according to the following formula:

$$DQ = \frac{\text{test region (patient sample)/control region (patient sample)}}{\text{test region (normal control sample)/control region (normal control sample)}}$$

Average DQ was determined for each subject patient and each positive control patient. Patients were considered as having an intragenic deletion if their average DQ was within the DQ range for deletion that was determined from average DQ of six positive controls ±2 SD.

Fluorescent in situ hybridization (FISH)

FISH was performed on metaphase chromosomes of a SoS patient (SoS 13). Plasmid DNA containing probe a, b, or c was labeled with biotin-16-dUTP (Roche Diagnostics, Mannheim, Germany) by nick translation at 37 °C for two hrs. A BAC clone, RP11-465I17, labeled with SpectrumOrange™-11-dUTP (Vysis, Downers Grove, IL) was used as a control. Probes a, b and c, and the control probe were combined with human Cot-1 and salmon sperm DNAs in a hybridization mixture, denatured at 70 °C for 10 min, applied on the chromosomes, and incubated at 37 °C for 72 hrs. Slides were washed, and solutions containing avidin D FITC, biotinilated anti-avidin D antibody (Vector Laboratories, Burlingame, CA), and again avidin D FITC were serially mounted on slides at 37 °C each for 15 min, and washed again. Finally, slides were mounted with an antifade solution (Vector Laboratories, Burlingame, CA) containing DAPI. Fluorescence photomicroscopy was performed as described previously.[13]

Results

NSD1-specific exon array CGH

We hybridized Cy3-labeled male and Cy5-labeled female control DNAs to the *NSD1*-specific microarray DNA. The Cy5/Cy3 signal ratios of all array elements of the *NSD1* locus as well as of three chromosome-13 elements were within the normal range, indicating no difference in the copy-number between the two controls. The Cy5/Cy3 ratios for three X-chromosome elements were higher than the +3 SD value, clearly reflecting copy-number difference in X chromosome (Figure 2 A). When hybridized with Cy3-labeled DNA from a male patient (SoS 3) who has a confirmed 5q35 whole-gene microdeletion, and with Cy5-labeled female control DNA, the Cy5/Cy3 ratios for the *NSD1* elements and X-chromosome elements were higher than the +3 SD value, the result indicating a deletion of the entire *NSD1* region (Figure 2 B). The Cy5/Cy3 ratios for chromosome-13 elements remained within the normal range, the result corresponding to normal choromosome-13 karyotype in both DNA samples.

Array CGH for DNA from the 30 patients without a whole-*NSD1* gene microdeletion or an *NSD1* intragenic mutation showed two patterns: A pattern of the normal ratio for all elements at the entire *NSD1* locus in 14 patients (Figure 2 C), and a possible pattern of deletion involving the 5' upstream region (elements 5'-1, 5'-2, 5'-3, 5'-4, and 5'-5) and exons 1 and 2 of *NSD1* in 16 patients (Figure 2 D).

QFD-PCR and FISH

To confirm the suspected copy-number changes of the 5' region of *NSD1* in 16 patients, QFD-PCR was performed (Figure 1). The region "A" (about 1.8 kb upstream of exon 1) was chosen for the analysis, because it showed high ratios in the microarray CGH analysis in all the 16 patients. Dosage ratios of the region "A" to the control region were evaluated in 28 patients (two patients were not evaluated as DNA was used up), six normal controls, and six other patients with confirmed 5q35 whole-gene microdeletions as positive controls. The DQ range for deletion determined from DQ values among the six positive controls was 0.16- 0.50 with the mean (SD) of 0.33 (0.08). In all but one patient (SoS13) examined, DQ was higher than 0.50 (Figure 3). These findings indicated that 15 of the 16 patients are unlikely to possess a deletion. FISH using combined probes a, b and c (Figure 1) was performed on metaphase chromosomes of SoS 13. Signal was observed on the long arm of both chromosomes 5 (Figure 4), indicating that SoS 13 did not have a deletion.

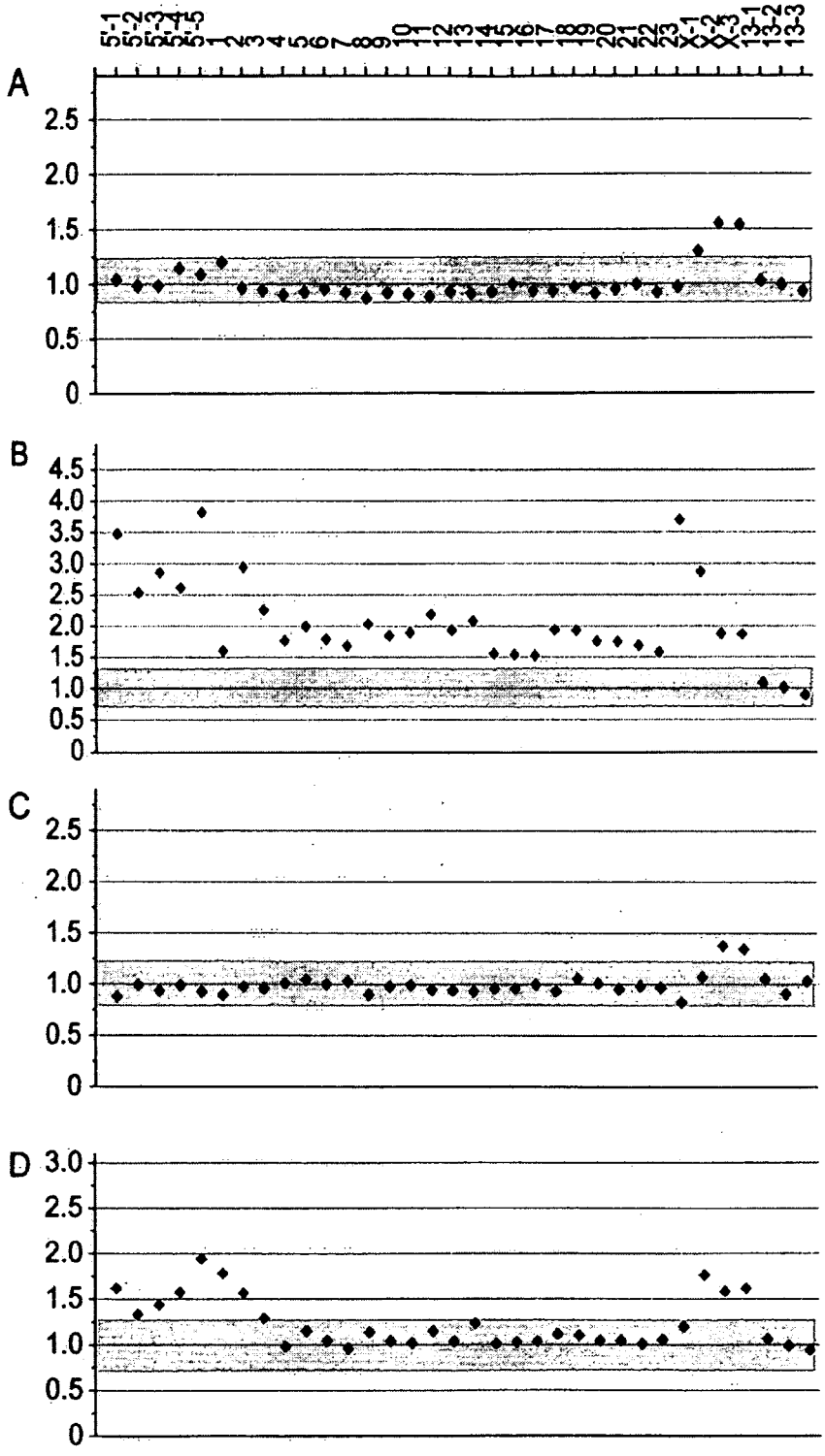

Figure 2. *NSD1* exon array CGH. The Cy5/Cy3 ratios are indicated on the y-axis. Range of ±3 SD is represented as gray area. **A.** Hybridization of normal male control DNA (Cy3) and normal female control DNA (Cy5). Note that the Cy5/Cy3 ratios of three elements of chromosome X are higher than the +3 SD value. **B.** Hybridization of SoS3 (with confirmed *NSD1* deletion) DNA (Cy3) and normal female control DNA (Cy5). Note that the Cy5/Cy3 ratios for all array elements except those of chromosome 13 are higher than the +3 SD value. **C.** Hybridization of SoS30 DNA (Cy5) and normal male DNA (Cy3). This is an example of a "normal" pattern seen in 14 out of 30 SoS patients. **D.** Hybridization of SoS13 DNA (Cy3) and normal female control DNA (Cy5). This is an example of a possible deletion pattern observed in 16 out of 30 SoS patients. Note that the Cy5/Cy3 ratios of 5'-1, 5'-2, 5'-3, 5'-4, 5'-5, 1, and 2 elements are higher than the +3 SD value, suggesting an abnormality at the 5' region of *NSD1*.

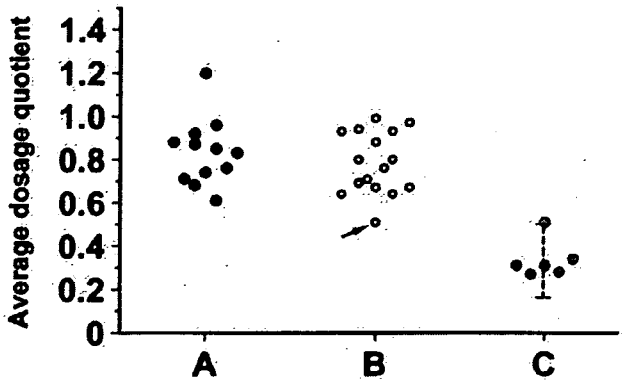

Figure 3. Confirmatory quantitative fluorescent duplex PCR. Average dosage quotients (DQs) for three groups of patients are shown: those with normal array CGH results (group A); those with suspected deletion (group B); and those with confirmed whole-gene microdeletion by FISH (group C). Possible deletion range (0.16-0.50) is shown by vertical bar. Note that average DQ in SoS13 (shown by arrow) is at the border of the deletion range.

Figure 4. FISH on metaphase chromosomes of SoS 13. Arrowheads indicate signals from the control probe (RP11-465I17). Arrows show signals of combined probes a, b and c, which are visible on both chromosomes 5.

Discussion

Results of *NSD1*-specific exon array CGH suggested that the 5' region of *NSD1* might be deleted in 16 of 30 SoS patients analyzed. However, in none of them, the subsequent QFD-PCR confirmed such an abnormality. Moreover, FISH analysis never proved a deletion in SoS 13. Therefore, intragenic deletions were ruled out as a possible genetic cause in our series of 30 Japanese SoS patients without any *NSD1* point mutations or whole-gene microdeletions. Douglas et al. suggested that Alu mediated recombination leading to partial deletions would be the likely cause in some of European patients,[11] but we could not find such partial deletions in Japanese patients.

Exon-based array CGH has been successful in detecting copy-number changes.[16,17] Our *NSD1*-specific microarray covered all 23 exons as well as five regions in an 18-kb segment upstream of exon 1, where two CpG islands are located (according to UCSC genome browser). We cloned all probes necessary for PCR for the regions, and the use of a single set of 5'-amino-linked primers simplified further amplification of inserts. Although our system worked well in hybridization of normal and positive controls, seemingly positive results recognized in 16 of 30 patients on probes of 5'-1, 5'-2, 5'-3, 5'-4, 5'-5 and exons 1-2, were later denied by QFD-PCR and FISH analyses, though either QFD-PCR or FISH system did not cover all the areas with positive results in exon arrays. These false positive data may be explained by different nucleotide contents within the microarray elements used. The average CG content in the elements of a proximal 20-kb region (5'-1 to 2) of *NSD1* (Figure 1) is 54 % with the maximum of 74 % within exon 1, while it is only 39 % in elements from exon 3 to exon 23. High CG contents could affect efficiency of hybridization and washing of labeled probes. Also, as elements of the exon microarray are much smaller in size than those of BAC-clone microarray and have much less DNA complexity, they are likely to be more affected by sequence contents.

Since *NSD1* intragenic deletions are less frequent in Japanese patients with SoS, other disease-causing mechanisms must be considered. A mutation screening of *NSD2* and *NSD3* that belong to the same family as *NSD1* failed to identify any aberrations in 78 patients with overgrowth syndromes, including 12 typical SoS patients without *NSD1* mutations,[18] therefore excluding *NSD2* and *NSD3* as candidacy. In addition, epigenetic changes may be important. Two SoS patients without *NSD1* aberrations have been reported to have abnormities in 11p15, the region which contains two imprinting domains related to Beckwith-Wiedemann Syndrome (OMIM #130850).[19] One case had paternal isodisomy for chromosome 11 and showed demethylation of *KCNQ1OT*, and the other exhibited partial *KCNQ1OT* demethylation. However, additional patients with such imprinting defects have not been reported. Hypermethylation or a mutation in the promoter region of *NSD1* as another possible cause was ruled out in 18 Japanese patients.[20]

In conclusion, intragenic deletion was not identified in our series of 30 Japanese patients with SoS. Therefore, the cause in approximately one third of Japanese SoS patients still remains unexplained. Other genetic aberrations that impair function of the components of *NSD1*-related pathway could be associated with a subset of SoS patients. Finally, exon array CGH is potentially useful, but shorter array elements may be easily affected by sequence contents, therefore data should carefully be evaluated.

Acknowledgements

This study was supported in part by Grants-in-Aid for Scientific Research No. 18390108 for N.M. and No. 17019055 (Priority Area "Applied Genomics") for N.N. from the Ministry of Education, Culture, Sports, Science and Technology of Japan.

References

1. Kurotaki N, Imaizumi K, Harada N et al. Haploinsufficiency of NSD1 causes Sotos syndrome. *Nat Genet* 30: 365-366, 2002
2. Kamimura J, Endo Y, Kurotaki N et al. Identification of eight novel NSD1 mutations in Sotos syndrome. *J Med Genet* 40: e126, 2003
3. Kurotaki N, Harada N, Shimokawa O et al. Fifty microdeletions among 112 cases of Sotos syndrome: low copy repeats possibly mediate the common deletion. *Hum Mutat* 22: 378-387, 2003
4. Cecconi M, Forzano F, Milani D et al. Mutation analysis of the NSD1 gene in a group of 59 patients with congenital overgrowth. *Am J Med Genet* A 134: 247-253, 2005
5. de Boer L, Kant SG, Karperien M et al. Genotype-phenotype correlation in patients suspected of having Sotos syndrome. *Horm Res* 62: 197-207, 2004
6. Douglas J, Hanks S, Temple IK et al. NSD1 mutations are the major cause of Sotos syndrome and occur in some cases of Weaver syndrome but are rare in other overgrowth phenotypes. *Am J Hum Genet* 72: 132-143, 2003
7. Rio M, Clech L, Amiel J et al. Spectrum of NSD1 mutations in Sotos and Weaver syndromes. *J Med Genet* 40: 436-440, 2003
8. Tatton-Brown K, Douglas J, Coleman K et al. Genotype-phenotype associations in Sotos syndrome: an analysis of 266 individuals with NSD1 aberrations. *Am J Hum Genet* 77: 193-204, 2005
9. Tong TM, Hau EW, Lo IF, Chan DH, Lam ST. Spectrum of NSD1 gene mutations in southern Chinese patients with Sotos syndrome. *Chin Med J (Engl)* 118:1499-1506, 2005
10. Turkmen S, Gillessen-Kaesbach G, Meinecke P et al. Mutations in NSD1 are responsible for Sotos syndrome, but are not a frequent finding in other overgrowth phenotypes. *Eur J Hum Genet* 11: 858-865, 2003
11. Douglas J, Tatton-Brown K, Coleman K et al. Partial NSD1 deletions cause 5% of Sotos syndrome and are readily identifiable by multiplex ligation dependent probe amplification. *J Med Genet* 42: e56, 2005
12. Fiegler H, Carr P, Douglas EJ et al. DNA microarrays for comparative genomic hybridization based on DOP-PCR amplification of BAC and PAC clones. *Genes Chromosomes Cancer* 36: 361-374, 2003
13. Harada N, Hatchwell E, Okamoto N et al. Subtelomere specific microarray based comparative genomic hybridisation: a rapid detection system for cryptic rearrangements in idiopathic mental retardation. *J Med Genet* 41: 130-136, 2004
14. Morgan NV, Tipping AJ, Joenje H, Mathew CG. High frequency of large intragenic deletions in the Fanconi anemia group A gene. *Am J Hum Genet* 65: 1330-1341, 1999
15. Yau SC, Bobrow M, Mathew CG, Abbs SJ. Accurate diagnosis of carriers of deletions and duplications in Duchenne/Becker muscular dystrophy by fluorescent dosage analysis. *J Med Genet* 33: 550-558, 1996
16. Dhami P, Coffey AJ, Abbs S et al. Exon array CGH: detection of copy-number changes at the resolution of individual exons in the human genome. *Am J Hum Genet* 76: 750-762, 2005
17. Frolov A, Prowse AH, Vanderveer L, Bove B, Wu H, Godwin AK. DNA array-based method for detection of large rearrangements in the BRCA1 gene. *Genes Chromosomes Cancer* 35: 232-241, 2002
18. Douglas J, Coleman K, Tatton-Brown K et al. Evaluation of NSD2 and NSD3 in overgrowth syndromes. *Eur J Hum Genet* 13: 150-153, 2005.
19. Baujat G, Rio M, Rossignol S et al. Paradoxical NSD1 mutations in Beckwith-Wiedemann syndrome and 11p15 anomalies in Sotos syndrome. *Am J Hum Genet* 74: 715-720, 2004
20. Visser R, Hasegawa T, Niikawa N, Matsumoto N. Analysis of the NSD1 promoter region in patients with a Sotos syndrome phenotype. *J Hum Genet* 51: 15-20, 2006

INTERNAL MEDICINE

□ CASE REPORT □

A Japanese Family of Typical Loeys-Dietz Syndrome with a TGFBR2 Mutation

Yosuke Togashi[1], Hiroto Sakoda[1], Akira Nishimura[2], Naomichi Matsumoto[2], Hisatoyo Hiraoka[1] and Yuji Matsuzawa[1]

Abstract

This report describes a Japanese family with vessel and craniofacial abnormalities. Although the clinical findings of the patient's father fulfilled the diagnostic criteria for Marfan syndrome, arterial tortuosity, aneurysms, hypertelorism and a bifid uvula were noted in both the patient and his father. These findings were compatible with the clinical manifestations that were previously reported in Loeys-Dietz syndrome. A molecular genetic analysis demonstrated a heterozygous missense mutation of the transforming growth factor-beta receptor II gene in both the patient and his father, which thus caused Loeys-Dietz syndrome. This is the first Japanese family case report of typical Loeys-Dietz syndrome.

Key words: aortic aneurysm and dissection, arterial tortuosity, Loeys-Dietz syndrome, transforming growth factor-beta receptor, Marfan syndrome

(DOI: 10.2169/internalmedicine.46.0467)

Introduction

Marfan syndrome (MFS) is an autosomal dominant connective tissue disorder. Classic MFS clinically presents cardinal features including skeletal, ocular and cardiovascular abnormalities, and most cases of MFS are caused by fibrillin-1 gene (FBN1) mutations. Recently, transforming growth factor-beta (TGF-beta) receptor II gene (TGFBR2) mutations were identified in a subset of patients with MFS; this syndrome was termed Marfan syndrome type 2 (MFS2) (1). A new dysmorphic syndrome with mutations in either transforming growth factor-beta receptor I gene (TGFBR1) or TGFBR2 was reported as Loeys-Dietz syndrome (LDS) (2), characterized by hypertelorism (widely spaced eyes), cleft palate or bifid uvula, aortic root aneurysm, arterial tortuosity and aneurysms of other vessels. This report describes a Japanese family who presented with the typical manifestations of LDS associated with a TGFBR2 mutation.

Case Report

A 24-year-old man visited the hospital for examination of his cardiovascular system because there was a history of cardiovascular disease in his family. His father presented with an acute ascending aortic aneurysm and dissection at 45 years of age in spite of normotension and underwent graft replacement of the ascending aorta and transverse aortic arch. In the following year, he underwent elective surgical repair of the descending aorta because the false lumen had dilated rapidly. His grandfather died suddenly in his early 30s from an unknown cause. His uncle also died suddenly in his early 20s from an acute aortic aneurysm and dissection. These events suggested that he was a presymptomatic patient of MFS based of his family history (Fig. 1).

The patient was a 176 cm tall and 75 kg man. He had a past history of a right hemifacial spasm at 20 years of age. A detailed physical examination revealed joint hypermobility, pectus excavatum, retrognathia and scoliosis. However, no cardiovascular findings, ocular findings nor lumbosacral dural ectasia were observed. The diagnostic criteria for MFS (the Ghent criteria) were not fulfilled clinically, although the patient had hypertelorism and a bifid uvula (Fig. 2A,B). Carotid ultrasonography and magnetic resonance angiography (MRA) demonstrated a carotid aneurysm and arterial tortu-

[1]Department of Internal Medicine, Sumitomo Hospital, Osaka and [2]Department of Human Genetics, Yokohama City University Graduate School of Medicine, Yokohama

Received for publication July 24, 2007; Accepted for publication September 8, 2007

Correspondence to Dr. Yosuke Togashi, togashi-yousuke@sumitomo-hp.or.jp

DOI: 10.2169/internalmedicine.46.0467

osity (Fig. 2C-F). These findings were consistent with the clinical manifestations of LDS (Table 1).

The patient's father was a 179 cm tall and 61 kg man. In addition to the previous history of the aortic aneurysm and dissection, the patient's father presented with a left hemifacial spasm at 43 years of age, cerebral infarction and diabetes at 54 years of age. A physical examination revealed joint hypermobility, retrognathia, scoliosis and striae atrophicae. Computed tomography (CT) and echocardiography demonstrated lumbosacral dural ectasia, apical blebs and Valsalva sinus dilation, but no significant ocular findings were recognized. In addition, his father also had hypertelorism and a bifid uvula (Fig. 3A,B). Carotid ultrasonography and MRA demonstrated carotid aneurysms and cerebral arterial tortuosity (Fig. 3C-F). The findings of a physical examination and imaging studies were indicative of LDS, whereas MFS was also considered to be a possibility (Table 1).

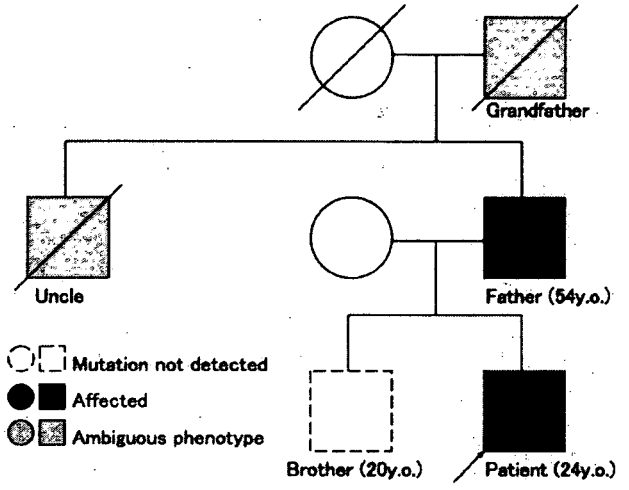

Figure 1. The pedigree of the family. The patient's father presented with an acute ascending aortic aneurysm and dissection at 45 years of age. His grandfather died suddenly in early 30s from an unknown cause, and his uncle also died suddenly in early 20s from an aortic aneurysm and dissection.

These clinical manifestations and the family history suggested that they had LDS. After obtaining informed consent from the family members, DNA sequencing of the TGFBR1 and TGFBR2 loci was conducted to identify mutations linked to LDS. A heterozygous missense mutation of TGFBR2 (1438C>T, Arg495Stop, Ex6) was detected in both the patient and his father (Fig. 4). This mutation has been previously described in LDS (3). Both the patient and his father were subsequently diagnosed to have LDS with a TGFBR2 mutation.

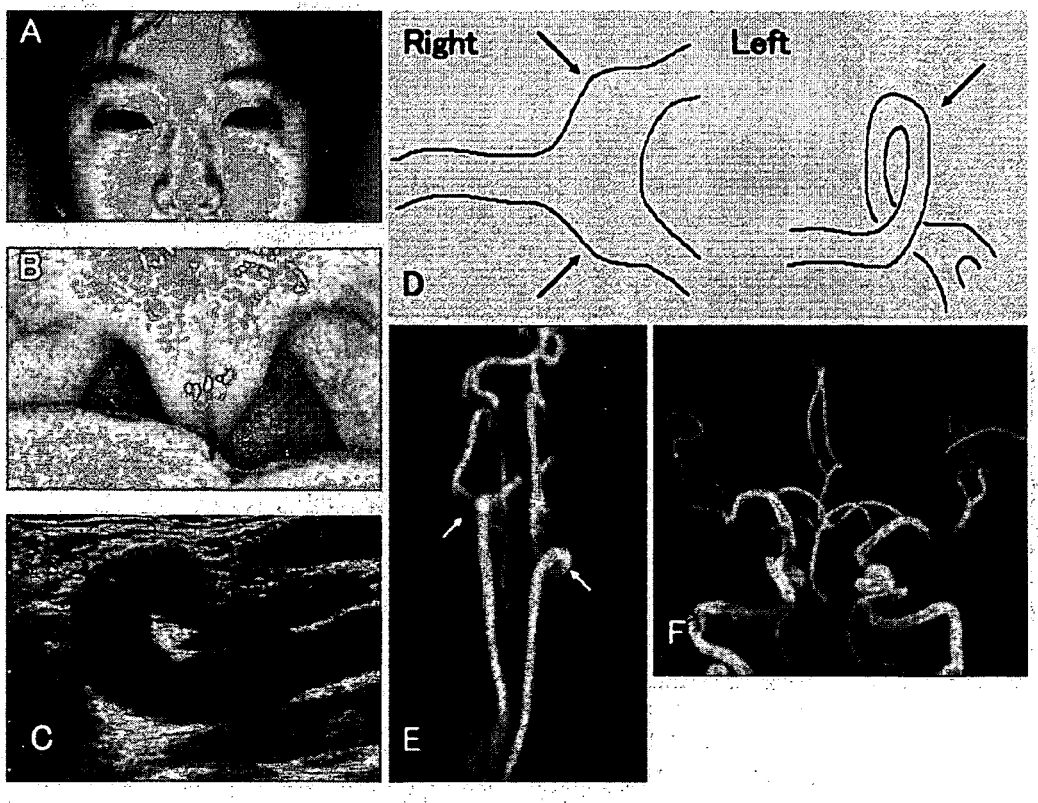

Figure 2. The clinical findings of the patient. A: Hypertelorism. B: Bifid uvula (arrow). C: Carotid ultrasonography showing a left common carotid artery loop. D: A carotid aneurysm and arterial tortuosity visualized by carotid ultrasonography (arrows). The left common carotid artery formed a loop. E: Carotid MRA showing a right carotid aneurysm and a left common carotid artery loop (arrows). F: Cerebral MRA showing cerebral arterial tortuosity.

DOI: 10.2169/internalmedicine.46.0467

Table 1. Clinical Manifestations of Loeys-Dietz Syndrome in the Patient and His Father with the Same TGFBR2 Mutation

*Reported by Loeys et al. (2)

	The patient	His father	Frequency of LDS*	Marfan syndrome*
Hypertelorism	+	+	93%	Not associated
Cleft palate or bifid uvula	+	+	100%	Not associated
Aortic root aneurysm	-	+	100%	Typical
Arterial tortuosity	+	+	100%	Not associated
Aneurysm of other vessels	+	+	92%	Rare
Craniosynostosis	-	-	36%	Not associated
Malar hypoplasia	-	-	85%	Associated
Blue sclerae	-	-	62%	Not associated
Ectopia lentis	-	-	0%	Typical
Arachnodactomy	-	-	57%	Typical
Dolichostenomelia	-	-	29%	Typical
Pectus deformity	-	-	64%	Typical
Scoliosis	+	+	71%	Typical
Talipes equinovarus	-	-	29%	Not associated
Camptodactyly	+	+	43%	Associated
Joint laxity	+	+	86%	Typical
Patent ductus arteriosus	-	-	54%	Not associated
Aterial septal defect	-	-	31%	Not associated
Chiari type 1	-	-	20%	Not associated
Developmental delay	-	-	21%	Not associated
Hydrocephalus	-	-	15%	Not associated

Discussion

MFS is an autosomal dominant connective tissue disorder with a reported incidence of 1 in 5000 to 10000 individuals. About 25% of MFS cases are sporadic due to de-novo mutations (4). Classic features include skeletal manifestations (pectus carinatum, scoliosis, dolichostenomelia, arachnodactyly, joint hypermobility and a high arched palate), ocular complications (ectopia lentis, flat cornea, hypoplastic iris and hypoplastic ciliary muscle) and cardiovascular defects (ascending aortic aneurysms, aortic dissections and mitral valve abnormalities). Its diagnosis is usually made according to the Ghent criteria revised in 1996 (5).

The mutation of FBN1, encoding the matrix protein fibrillin-1, was identified in classic MFS in 1991 (6). FBN1 mutations are detected in 91-93% of MFS cases fulfilling the Ghent criteria (7). In 2004, TGFBR2 mutations were identified in patients with a second type of MFS not linked to FBN1 mutations, which was called Marfan syndrome type 2 (MFS2) (1). From a recent report, TGFBR mutations may account for approximately 5-10% of patients with MFS (8). In 2005, a new dysmorphic syndrome caused by mutations in either TGFBR1 or TGFBR2 was reported as Loeys-Dietz syndrome (LDS) (2). LDS is characterized by hypertelorism, cleft palate or bifid uvula, aortic root aneurysm, arterial tortuosity and aneurysms of other vessels. TGFBR mutations were also detected in patients with familial thoracic aortic aneurysms and dissections (9) and vascular type Ehlers-Danlos syndrome without the characteristic type III collagen abnormalities (3). Various phenotypes of cardiovascular syndrome with systemic involvement have been documented to be closely associated with TGFBR mutations.

The patient and his father were diagnosed to have LDS based on their clinical findings (Table 1) and the presence of a TGFBR2 mutation. This is the first Japanese family case report of LDS with typical clinical manifestations, although, several Japanese cases with MFS and MFS-related disorders caused by TGFBR mutations, including LDS, were previously reported (1, 8, 10). Some clinical features of MFS, MFS2 and LDS are markedly overlapped, but it is important that no significant ocular findings are observed in MFS2 and LDS caused by TGFBR mutations, as was observed in this patient's family. It is highly debatable whether MFS2 with TGFBR mutations can be clearly distinguished from LDS. Loeys et al have argued that some characteristic features of LDS such as bifid uvula, skin findings and arterial tortuosity might be overlooked on examination of a suspected MFS family. A comprehensive clinical evaluation including DNA analysis for TGFBR mutations is critical for the diagnosis of LDS (3).

It is notable that the present patient and his father had suffered from hemifacial spasms. Vascular abnormalities of LDS may be causally related to this facial nerve disorder

DOI: 10.2169/internalmedicine.46.0467

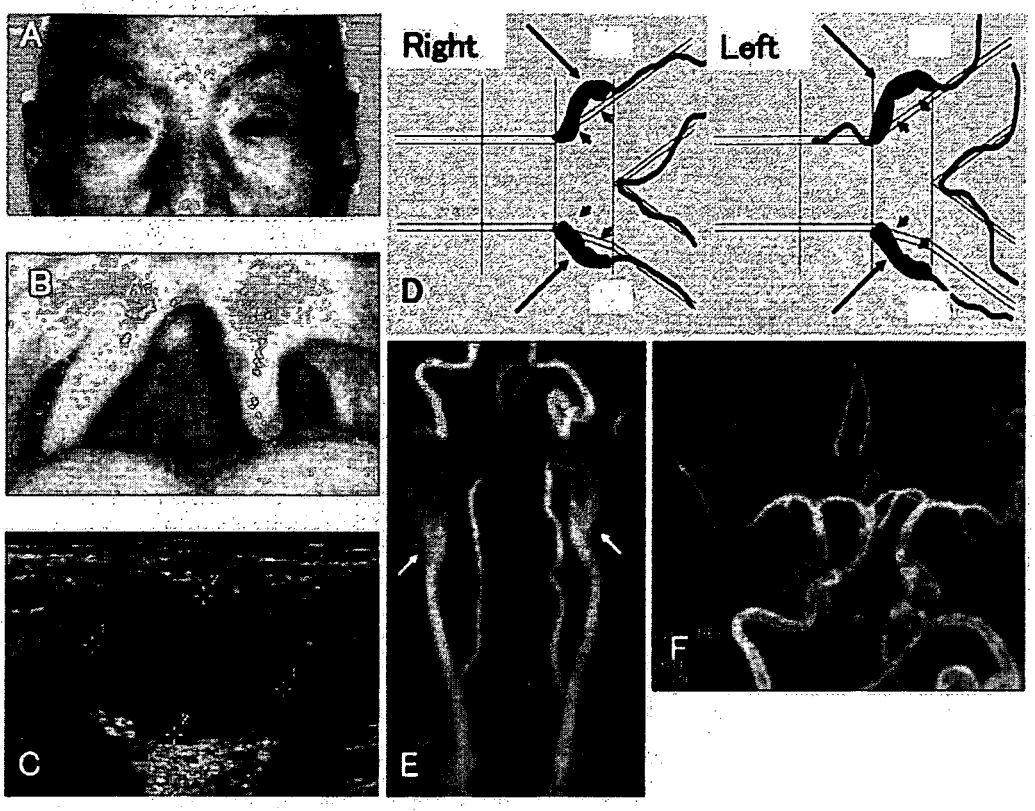

Figure 3. The clinical findings of the patient's father. A: Hypertelorism. B: Bifid uvula (arrow). C: Carotid ultrasonography showing a right carotid aneurysm. D: Bilateral carotid aneurysms visualized by carotid ultrasonography (long arrows). Atherosclerotic plaques were detected in the aneurysms (short arrows). E: Carotid MRA showing bilateral carotid aneurysms (arrows). F: Cerebral MRA showing cerebral arterial tortuosity.

because tortuous arteries might be compressing the facial nerve. Furthermore, his father had repeated episodes of cerebral infarction, which might be also caused by blood clots presumably from carotid aneurysms and tortuous arteries. These neurological findings may be helpful signs of vascular abnormalities of the head and neck in LDS patients.

The histopathological findings in MFS are accounted for by the FBN1 mutations. In addition to the structural role of fibrillin-1, it may also have a critical role in the regulation of TGF-beta signaling (4). Support for this hypothesis is seen in mouse models of MFS. Transgenic mice with FBN1 mutations display several MFS features with variable severity (11-13) and increased TGF-beta signaling is observed in at least four organs (i.e. lung, mitral valve, aortic and dural tissues) (14-17). Administration of anti-TGF-beta neutralizing antibody (NAb) rescued these tissue phenotypes (14, 16, 17). Mice homozygous for a hypomorphic FBN1 allele have impaired pulmonary alveolar septation associated with increased TGF-beta signaling, that can be prevented by the administration of TGF-beta NAb (16). Similarly, myxomatous thickening of the mitral valve and aortic root dilation in mice harboring FBN1 mutations are also attenuated by the administration of TGF-beta NAb (14, 17). Furthermore, aortic aneurysm was prevented with the use of losartan, an angiotensin II type 1 receptor blocker, that reduces increased TGF-beta signaling (14). In addition, mutation analysis in Camurati-Engelmann disease (CED), characterized by marfanoid skeletal abnormalities, identified TGF-beta 1 gene mutations. Increased TGF-beta 1 activity, which is seen in CED patients, is expected to inhibit muscle and fat development (18). TGF-beta signaling may play an important role in the formation of cardiovascular system and skeletal structures. The TGFBR mutations identified in MFS and MFS-related disorders including LDS probably increase TGF-beta signaling, which causes multiple organ connective tissue disorders.

The TGF-beta superfamily is composed of many multifunctional cytokines, including TGF-betas, bone morphogenetic proteins (BMPs), activins, inhibins, and mycostatin. They participate in a wide range of processes, from tissue differentiation during development through to regulation of mesenchymal and immune cell functions. They are expressed by cells in the vessel wall and are capable of modulating vascular development and remodeling by altering cell differentiation, proliferation, migration, extracellular matrix production, and the activities of immune cells (19). Subsequently, the effects of TGF-beta signaling on the cardiovascular system has become increasingly clear, which may elucidate the pathophysiological processes of LDS with TGFBR mutations and provide likely avenues for future re-

DOI: 10.2169/internalmedicine.46.0467

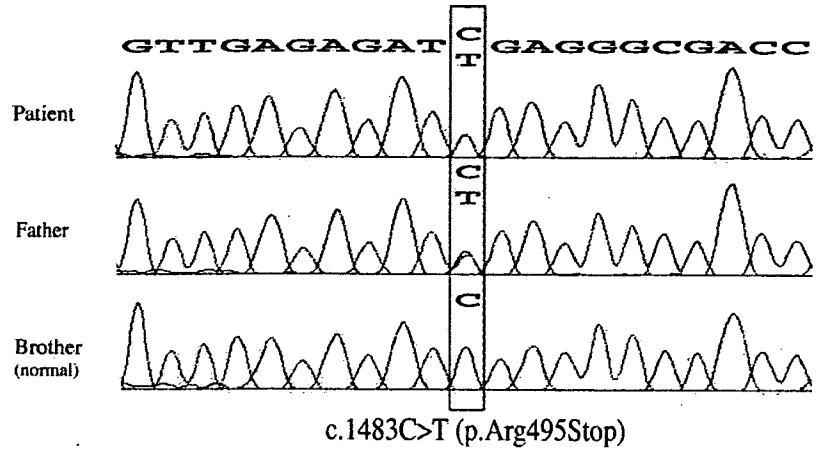

Figure 4. TGFBR2. The heterozygous missense mutation of TGFBR2 was detected in both the patient and his father. This mutation was not detected in his brother who also demonstrated no clinical manifestations of LDS.

search that may lead to novel pharmacological therapies for the treatment or prevention of critical vascular disorders.

In patients with the classic MFS, the life span of untreated patients was about 32 years in 1972 and improved therapy has resulted in a marked increase in life expectancy to 41 years in 1993 and to 61 years in 1995 (20, 21). On the other hand, MFS and MFS-related disorders caused by TGFBR mutations, including LDS, are predisposed to severe vascular consequences at a young age (22). Since the natural histories of LDS are considerably distinct from those of MFS caused by FBN1 mutations, Loeys et al emphasize the importance of comprehensive diagnostic clinical evaluation and the efficacy of genetic analysis for TGFBR mutations to identify the LDS patients (3). The affected patients have a high risk for arterial dissection without marked arterial dilatation, so that aggressive surgical repair of arterial aneurysms may be considered independent of age because the very low intraoperative mortality rate (3, 23-25). Although the patient is asymptomatic and maintains good health, clinical assessment with periodic physical examination and cardiovascular imaging procedures (e.g. ultrasonography, CT scans and MRI) is required to prevent serious cardiovascular events in the future.

This article describes a Japanese family who presented with typical manifestations of LDS with a TGFBR2 mutation. Some clinical features are markedly overlapped in MFS and LDS. Patients with marfan-like symptoms who present with craniofacial features of hypertelorism and bifid uvula, and vascular abnormalities characterized by arterial tortuosity and aneurysms, should be considered as those with the Loeys-Dietz syndrome. Since there are very few LDS cases reported to date in Japan, epidemiologic surveillance of Japanese LDS families is urgently required in order to clarify the optimal management of vascular complications.

References

1. Mizuguchi T, Collod-Beroud G, Akiyama T, et al. Heterozygous TGFBR2 mutations in Marfan syndrome. Nat Genet **36**: 855-860, 2004.
2. Loeys BL, Chen J, Neptune ER, et al. A syndrome of altered cardiovascular, craniofacial, neurocognitive and skeletal development caused by mutations in TGFBR1 or TGFBR2. Nat Genet **37**: 275-281, 2005.
3. Loeys BL, Schwarze U, Holm T, et al. Aneurysm syndromes caused by mutations in the TGF-beta receptor. N Engl J Med **355**: 788-798, 2006.
4. Judge DP, Dietz HC. Marfan's syndrome. Lancet **366**: 1965-1976, 2005.
5. De Paepe A, Devereux RB, Dietz HC, Hennekam RC, Pyeritz RE. Revised diagnostic criteria for the Marfan syndrome. Am J Med Genet **62**: 417-426, 1996.
6. Dietz HC, Cutting GR, Pyeritz RE, et al. Marfan syndrome caused by a recurrent de novo missense mutation in the fibrillin gene. Nature **352**: 337-339, 1991.
7. Loeys B, De Backer J, Van Acker P, et al. Comprehensive molecular screening of the FBN1 gene favors locus homogeneity of classical Marfan syndrome. Hum Mutat **24**: 140-146, 2004.
8. Sakai H, Visser R, Ikegawa S, et al. Comprehensive genetic analysis of relevant four genes in 49 patients with Marfan syndrome or Marfan-related phenotypes. Am J Med Genet A **140**: 1719-1725, 2006.
9. Pannu H, Fadulu VT, Chang J, et al. Mutations in transforming growth factor-beta receptor type II cause familial thoracic aortic aneurysms and dissections. Circulation **112**: 513-520, 2005.
10. Akutsu K, Morisaki H, Takeshita S, et al. Phenotypic Heterogeneity of Marfan-Like Connective Tissue Disorders Associated With Mutations in the Transforming Growth Factor-beta Receptor Genes. Circ J **71**: 1305-1309, 2007.
11. Judge DP, Biery NJ, Keene DR, et al. Evidence for a critical contribution of haploinsufficiency in the complex pathogenesis of Marfan syndrome. J Clin Invest **114**: 172-181, 2004.
12. Pereira L, Andrikopoulos K, Tian J, et al. Targetting of the gene encoding fibrillin-1 recapitulates the vascular aspect of Marfan syndrome. Nat Genet **17**: 218-222, 1997.

DOI: 10.2169/internalmedicine.46.0467

13. Pereira L, Lee SY, Gayraud B, et al. Pathogenetic sequence for aneurysm revealed in mice underexpressing fibrillin-1. Proc Natl Acad Sci U S A **96**: 3819-3823, 1999.
14. Habashi JP, Judge DP, Holm TM, et al. Losartan, an AT1 antagonist, prevents aortic aneurysm in a mouse model of Marfan syndrome. Science **312**: 117-121, 2006.
15. Jones KB, Myers L, Judge DP, Kirby PA, Dietz HC, Sponseller PD. Toward an understanding of dural ectasia: a light microscopy study in a murine model of Marfan syndrome. Spine **30**: 291-293, 2005.
16. Neptune ER, Frischmeyer PA, Arking DE, et al. Dysregulation of TGF-beta activation contributes to pathogenesis in Marfan syndrome. Nat Genet **33**: 407-411, 2003.
17. Ng CM, Cheng A, Myers LA, et al. TGF-beta-dependent pathogenesis of mitral valve prolapse in a mouse model of Marfan syndrome. J Clin Invest **114**: 1586-1592, 2004.
18. Janssens K, Vanhoenacker F, Bonduelle M, et al. Camurati-Engelmann disease: review of the clinical, radiological, and molecular data of 24 families and implications for diagnosis and treatment. J Med Genet **43**: 1-11, 2006.
19. Bobik A. Transforming growth factor-betas and vascular disorders. Arterioscler Thromb Vasc Biol **8**: 1712-1720, 2006.
20. Finkbohner R, Johnston D, Crawford ES, Coselli J, Milewicz DM. Marfan syndrome. Long-term survival and complications after aortic aneurysm repair. Circulation **91**: 728-733, 1995.
21. Silverman DI, Burton KJ, Gray J, et al. Life expectancy in the Marfan syndrome. Am J Cardiol **75**: 157-160, 1995.
22. Mizuguchi T, Matsumoto N. Recent progress in genetics of Marfan syndrome and Marfan-associated disorders. J Hum Genet **52**: 1-12, 2007.
23. Yetman AT, Beroukhim RS, Ivy DD, et al. Importance of the clinical recognition of Loeys-Dietz syndrome in the neonatal period. Pediatrics **119**: 1199-1202, 2007.
24. LeMaire SA, Pannu H, Tran-Fadulu V, et al. Severe aortic and arterial aneurysms associated with a TGFBR2 mutation. Nat Clin Pract Cardiovasc Med **4**: 167-171, 2007.
25. Williams JA, Loeys BL, Nwakanma LU, et al. Early surgical experience with Loeys-Dietz: a new syndrome of aggressive thoracic aortic aneurysm disease. Ann Thorac Surg **83**: S757-763, 2007.

J Hum Genet (2007) 52:334–341
DOI 10.1007/s10038-007-0116-7

ORIGINAL ARTICLE

Paroxysmal kinesigenic choreoathetosis (PKC): confirmation of linkage to 16p11-q21, but unsuccessful detection of mutations among 157 genes at the PKC-critical region in seven PKC families

Taeko Kikuchi · Masayo Nomura · Hiroaki Tomita · Naoki Harada · Kazuaki Kanai · Tohru Konishi · Ayako Yasuda · Masato Matsuura · Nobumasa Kato · Koh-ichiro Yoshiura · Norio Niikawa

Received: 22 November 2006 / Accepted: 13 January 2007 / Published online: 14 February 2007

Abstract Paroxysmal kinesigenic choreoathetosis (PKC) is a paroxysmal movement disorder of unknown cause. Although the PKC-critical region (PKCCR) has been assigned to the pericentromeric region of chromosome 16 by several studies of families from various ethnic backgrounds, the causative gene has not yet been identified. In the present study, we performed linkage and haplotype analysis in four new families with PKC, as well as an intensive polymerase chain reaction (PCR) based mutation analysis in seven families for a total of 1,563 exons from 157 genes mapped around the PKCCR. Consequently, the linkage/haplotype analysis revealed that PKC was assigned to a 24-cM segment between *D16S3131* and *D16S408*, the result confirming the previously defined PKCCR, but being unable to narrow it down. Although the mutation analysis of the 157 genes was unsuccessful at identifying any mutations that were shared by patients from the seven families, two nonsynonymous substitutions, i.e., 6186C>A in exon 3 of *SCNN1G* and 45842A>G in exon 29 of *ITGAL*, which were segregated with the disease in Families C and F, respectively, were not observed in more than 400 normal controls. Thus, one of the two genes, *SCNN1G* and *ITGAL*, could be causative for PKC, but we were not able to find any other mutations that explain the PKC phenotype.

Keywords Paroxysmal kinesigenic choreoathetosis (PKC) · PKC-critical region · Linkage analysis · Mutation analysis · *SCNN1G* · *ITGAL*

T. Kikuchi · M. Nomura · N. Harada · K. Yoshiura (✉) · N. Niikawa
Department of Human Genetics, Nagasaki University Graduate School of Biomedical Sciences, Sakamoto 1-12-4, Nagasaki 852-8523, Japan
e-mail: kyoshi@nagasaki-u.ac.jp

T. Kikuchi
Department of Psychiatry, Nagasaki University Graduate School of Biomedical Sciences, Nagasaki, Japan

H. Tomita
Department of Psychobiology, Graduate School of Medicine, Tohoku University, Sendai, Japan

N. Harada
Kyushu Medical Science, Nagasaki, Japan

K. Kanai
Department of Neurology, Chiba University School of Medicine, Chiba, Japan

T. Konishi
Division of Pediatrics, Nagaoka Ryoikuen, Nagaoka, Japan

A. Yasuda
Department of Pediatrics, Japanese Red Cross Nagoya First Hospital, Nagoya, Japan

M. Matsuura
Section of Biofunctional Informatics, Graduate School of Allied Health Sciences, Tokyo Medical and Dental University, Tokyo, Japan

N. Kato
Department of Psychiatry, Faculty of Medicine, University of Tokyo, Tokyo, Japan

T. Kikuchi · M. Nomura · N. Harada · K. Yoshiura · N. Niikawa
Solution Oriented Research of Science and Technology (SORST), Japan Science and Technology Agency (JST), Kawaguchi, Japan

Introduction

Paroxysmal kinesigenic choreoathetosis (PKC; MIM 128200) is a paroxysmal movement disorder characterized by recurrent and brief attacks of unilateral or bilateral involuntary movements, including dystonic posturing, chorea, athetosis, and ballism, which are precipitated by the sudden onset of movements (Kato et al. 2006). The attacks can last as long as a few seconds to a few minutes, occur up to 100 times daily, but usually manifest in childhood or early adolescents, and commonly decrease with age. There is no loss of consciousness during these attacks. The attacks are responsive to anticonvulsants such as carbamazepine or phenytoin. Electroencephalogram (EEG) analysis demonstrates normal or nonspecific abnormalities. Neuroimaging and neuropathological studies resulted in unremarkable findings (Sadamatsu et al. 1999; Nagamitsu et al. 1999). The etiology and pathophysiology of PKC still remain unclear. Some neurologists consider PKC as a form of reflex epilepsy, whereas others believe that basal ganglia dysfunction may play a role in its cause (Kato et al. 2006). Most (40–70%) were familial cases in which PKC was transmitted in an autosomal dominant mode of inheritance with incomplete penetrance (Tomita et al. 1999; Valente et al. 2000). Males are affected more often than females, with an estimated ratio of 3–4:1 (Bhatia 1999).

We previously performed a genome-wide linkage and haplotype analysis in eight Japanese families with PKC and defined the disease locus within a 12.4-cM region between *D16S3093* and *D16S416* at 16p11.2-q12.1 (Tomita et al. 1999). This PKC-critical region (PKCCR) was confirmed by others (Bennett et al. 2000; Swoboda et al. 2000; Valente et al. 2000; Cuenca-Leon et al. 2002). In addition, mapped regions for other conditions probably allelic to PKC, such as infantile convulsions and paroxysmal choreoathetosis (ICCA; MIM 602066) and benign familial infantile convulsions (BFIC2; MIM 605751), shared with that for PKC (Lee et al. 1998; Hattori et al. 2000; Swoboda et al. 2000; Caraballo et al. 2001; Weber et al. 2004). Nevertheless, mutations in any genes within the PKCCR have remained uncovered.

Here, we describe the results of the mutation analyses of seven PKC families for a total of 157 genes located at or around the PKCCR, together with linkage/haplotype analysis of four newly identified families.

Materials and methods

Subjects

The subjects studied included seven families (Families A–G) with PKC. Two of them (Families F and G) corresponded respectively to Families 1 and 3 in our previous report (Tomita et al. 1999), and five other families (Families A–E, Fig. 1) were those which were newly collected. A total of 21 members, including 16 PKC patients from four of the five families (Families A–D), underwent a linkage and haplotype analysis. In addition, one of each affected individual (we further call them representative patients) chosen from all seven families was subjected to mutation analysis. Blood samples were collected from all participants after obtaining written informed consent, and the study protocol was approved by the Committee for Ethical Issues on Human Genome and Gene Analysis at Nagasaki University.

Genotyping and linkage analysis

Genomic DNA was isolated from the blood lysate of the 21 participants by phenol-chloroform extraction, followed by ethanol precipitation. To try to narrow down the PKCCR, we performed genotyping and haplotype analysis in the four newly collected PKC families, using 13 microsatellite markers (Table 1) located to a 36-cM region at 16p12-q21 to which PKC has been shown to be linked, as well as using three

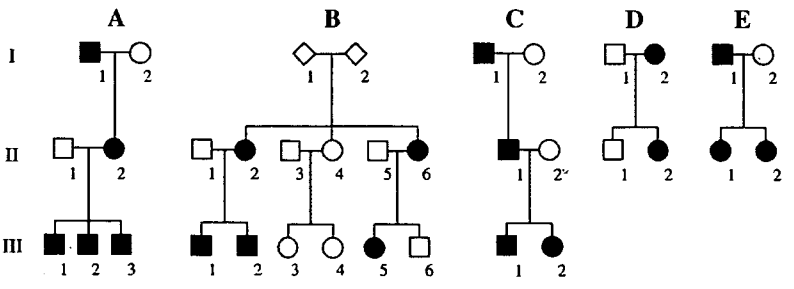

Fig. 1 Pedigree of the five families (Families A–E) with paroxysmal kinesigenic choreoathetosis (PKC). The *closed squares* and *circles* denote individuals affected with PKC. Although not shown here, Families F and G correspond to Families 1 and 3 reported previously (Tomita et al. 1999)

Table 1 Primer sequences of the 12 microsatellite markers used for genotyping and linkage analysis

Markers	Forward primer (5′–3′)	Reverse primer (5′–3′)
D16S403	CAAGACTAACGCTGATGGCT	GACAGTGAGGTGGGAATCAAA
D16S417	CTGTCCAACATGCAGCC	TGAAGTCAATCCCACTTGAA
D16S3131	CTGCTTCCATCTTGCC	CTAGCCCCCAAATGTG
D16S3093	CAAGGGCAAAACTCCAT	CCAAAAGGTTGATTCTCTG
AC007353-M1	GCTTAACTACATTTTATTCAAGGTTG	TCTGTGGTAGAGAGGCAAAGA
AC092368-M1	GTTTACCAGCCATTTTTAATCAACA	TGAATAAGTGTGTCTTTCAACAAAATT
AC092721-M3	GCCCTGTAATATAATTTGAAGTTG	GGGTTCAAGTGATTCTCCTG
D16S3136	CTCACCTATTGCCCTCAAGAA	CAGAATCTTATGCCATTATT
D16S416	CATAGGACCCTCAGATGTATA	CTGCCTATGGCTAAGAGGACA
D16S408	TGTAACCTTGTGTGCATCCT	CACTCTTATCCCAGGAACCC
D16S514	CAATTCCTTGATGCTACCAT	CTTGTCTAGTGGCTGGAATA
D16S3143	GCTACTGAGGAAACCTTATCC	GGCCATTACAGGAAGTGC

Primers of D16S3068 were purchased from the ABI PRISM Linkage Mapping Sets LMS (Applied Biosystems, Foster City, CA)

additional markers (AC007353-M1, AC092368-M1, and AC092721-M3) that were designed by us according to the human genome sequence (http://genome.cse.ucsc.edu/). Sample DNA was polymerase chain reaction (PCR) amplified for each marker locus with fluorescence-labeled primers. PCR was performed on DNA Thermal Cycler Model 9700 (Applied Biosystems, Foster City, CA) in a 10-μl reaction mixture containing 1×PCR buffer (Takara Bio, Otsu, Japan), 200 μM each of dNTP, 0.5 μM each of primer, 10 ng DNA, and 0.25 units ExTaq DNA polymerase HS-version (Takara Bio, Otsu, Japan) under the conditions of denaturation at 94°C for 2 min, 35 cycles of 94°C for 30 s, 58°C for 30 s, and 72°C for 1 min, and final extension at 72°C for 7 min. PCR products were run on an auto-sequencer Model 3100 (Applied Biosystems, Foster City, CA). Allele sizes were analyzed by GeneScan and Genotyper software (Applied Biosystems, Foster City, CA) to determine the genotypes.

Mutation analysis

We performed PCR-based mutation analysis of the seven representative patients with typical features of PKC. Sequences examined for mutations among the seven patients included those of 1,371 coding exons, excluding the 3′-UTR and 5′-UTR in 117 genes, located at the PKCCR between *D16S3093* and *D16S416* (Table 1). The analysis in five families (Families A and C–F) was expanded to an additional 192 exons of 40 other genes, whereas because of depletion of genomic DNA, an expanded analysis was not done in the remaining two families. Thus, a total of 1,563 exons in 157 genes were analyzed for mutation (primer sequences are available on request).

Real-time quantitative PCR

We performed real-time quantitative PCR in six representative patients from Families A and C–G. Six pairs of primers and TaqMan probes were designed for exons 1, 6, and 13 of *SCNN1G*, and for exons 1, 16, and 30 of *ITGAL*. PCR was carried out in a 10-μl reaction mixture containing 5 μl of 2×TaqMan Universal PCR Master mix (Applied Biosystems, Foster City, CA), 0.4 μM each of primer, a 0.2-μM probe, and 10 ng DNA under the conditions of 2 min at 50°C, 10 min at 95°C, 40 cycles of 15 s at 95°C, and 1 min at 60°C, with a 7900HT Sequence Detection System (Applied Biosystems, Foster City, CA).

Results

The haplotype analysis showed that all affected individuals in the four new families share an allele at each locus examined between *D16S3131* and *D16S408* (Fig. 2). One end of the shared region was defined by a recombination between *D16S3131* and *D16S3093* in individual III-3 in Family A, and the other end by a recombination between *D16S514* and *D16S408* in individual III-1 in the same family. These results defined a minimum PKCCR in the four new families within an approximately 24-cM segment between *D16S3131* and *D16S408*. Therefore, the present linkage/haplotype analysis did not contribute to narrow down the previously defined PKCCR.

Among a total of 1,563 exons of 157 genes analyzed, we detected 243 base alterations in the seven representative patients (Fig. 3), 36 of which were base substitutions in coding regions and have not been reported in the dbSNP database (http://www.ncbi.nlm.-

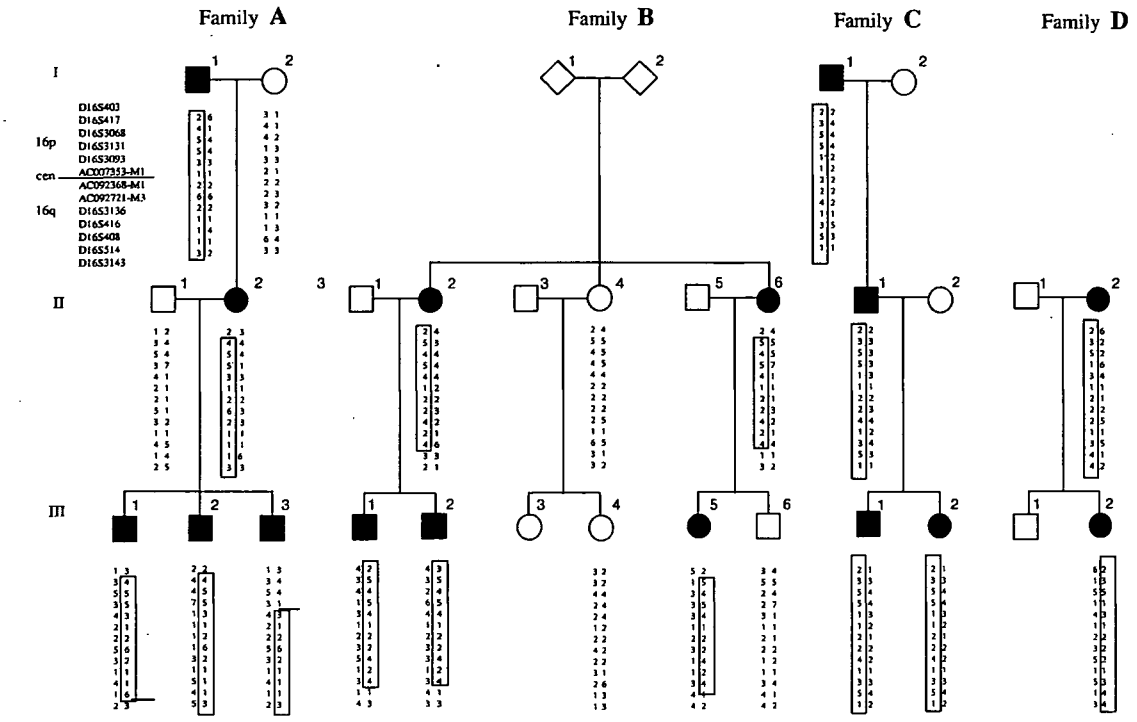

Fig. 2 Haplotype analysis of the four new PKC families (Families A–D). The *numbers in boxes* represent putative disease haplotypes. The *heavy short lines* indicate recombination sites

nih.gov/SNP/). Seven of the alterations in six genes were nonsynonymous substitutions resulting in amino-acid substitutions (Table 2). Five of such nonsynonymous substitutions in four genes were observed both in some patients and among 100 normal control individuals. The remaining two, i.e., 6186C>A in exon 3 of *SCNN1G* (the gene for sodium channel, nonvoltage-gated 1, gamma) and 45842A>G in exon 29 of *ITGAL* (the integrin alpha L precursor gene), observed in Families C and F, respectively, were not observed among more than 400 normal controls. The real-time quantitative PCR analysis did not detect a duplication or a deletion within the two genes. Of the 35 intronic base changes we identified in the seven patients, none were located at the acceptor or donor splice sites (Fig. 3).

G-banding chromosome analysis at the 400-band level and C-banding analysis revealed that all five patients from Families B–D, F, and G had a normal-sized heterochromatin block on chromosome 16 without an inversion (data not shown).

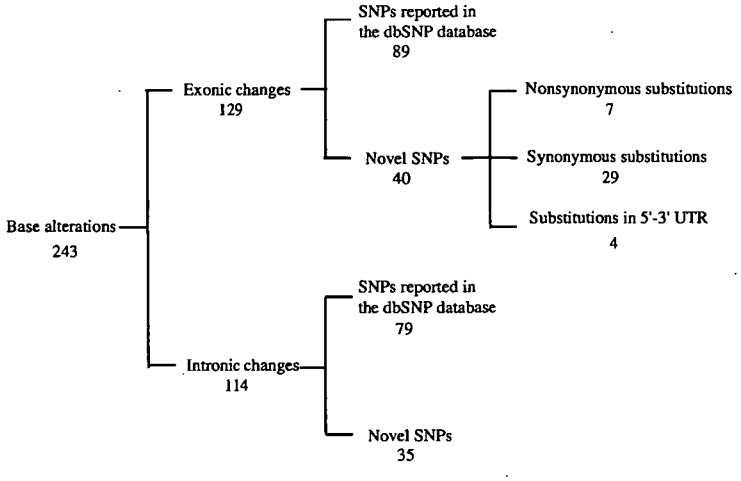

Fig. 3 Classification of 243 base alterations in 157 candidate genes. Information of the newly found single nucleotide polymorphisms (SNPs) is shown in Table 2. None of the novel intronic SNPs are located at any of the acceptor or donor splice sites

Table 2 List of genes for mutation analysis in the PKC patients, and novel SNPs identified, their positions, nucleotide changes, and amino acid changes

Gene	E/I	SNP definition	AA	Gene	E/I	SNP definition	AA	Gene	E/I	SNP definition	AA
HS3ST2*				ASPHD1	E1	515insTGG		ITGAX*			
SCNN1G*	E3	6185G>T	Y241Y	KCTD13*	I2	INV2-74A>T		ITGAD*	5′U	5′U-13G>C[a]	
	E3	6186C>A	P242T	LOC124446					E2	943C>T	G33G
SCNN1B*				TAOK2*					I7	INV7+38C>T	
UBPH*				HIRIP3*					E8	14188A>G	R246R
NDUFAB1*				CCDC95					E8	14253A>G	Y268C
PRKCB1*	E1	79C>A	R27R	DOC2A*					I9	INV10-43G>A	
	I15	INV15+85G>T		FAM57B	I2	INV2+66G>T			E16	19819A>G	S644G
CACNG3*				ALDOA*					I17	INV17+139G>A	
TNRC6A*	E1	5′U-12079T>A		PPP4C*	E1	5′U-355-347del(CGG)3			I19	INV19+71C>T	
	E21	33511C>T	H1551H	TBX6*					I27	INV27+87G>A	
SLC5A11*	I1	5′U-12193T>C		YPEL3*				ARMC5*			
	I2	INV2+6C>G		GDPD3				TGFB1I1*	E5	753C>T	P119S
	I5	INV5-30G>A		MAPK3*				SLC5A2*			
	I5	INV5+65T>C		CORO1A*				C16orf58*	I5	INV5+53G>A	
LCMT1*				SULT1A3*				ERAF*	3′U	3′U+570T>C[a]	
IL4R*	I3	INV3+72T>A		CD2BBP2*	I1	INV1+493C>T		MGC3020*			
	E11	22448T>C	L433L	TBC1D10B*				ZNF720*			
IL21R*	I4	INV4+51C>T		MYLPF	I5	INV5+27G>A		ZNF267			
GTF3C1*				SEPT1*				TP53TG3*	E3	1232insG	
KIAA0556*	I16	INV16+4T>C		ZNF553	E2	2434G>A	T326T	FLJ43855			
	E18	204044A>G	Q1198Q	ZNF771				POL3S			
GSGIL*				XTP3TPA*				FLJ46121			
XPO6*	I9	INV9+31insT		SEPHS2*				FLJ43980	E1	5′U-15C>G	
	I15	INV15+23G>C		ITGAL*	E1	5′U-86C>T		SHCBP1*	E5	12986C>T	N204N
	E16	69120T>C	N740N		E29	45842A>G	K1063R	VPS35*			
SBK-1				ZNE768				ORC6L	E6	6328A>G	V193V
LOC440350				ZNF747				MLCK*			
LOC440348				ZNF764				LOC388272*			
CLN3*	I12	INV12+36C>T		ZNF688				GPT2*			
	E15	14138A>G	H404R	ZNF785				DNAJA2*			
APOB48R*				ZNF689				NETO2*	I3	INV3-34G>A	
IL27*	I5	INV5-12C>T		PRR14				ITFG1 *			
NUPR1*				FBS1*				PHKB*	I28	INV28+37C>T	
CCDC101*				SRCAP*				ABCC12*			
SULTIA2*				PHKG2*				ABCC11*			
SULT1A1*				LOC90835				LONPL*			
EIF3S8*	E16	20499C>T	P725P	RNF40*				SIAH1			
ATXN2L*	I13	INV13+55G>A		BCL7C*				N4BP1*			
TUFM*				CTF1*				CBLN1*			
SH2B*				LOC283932				FLJ44674	E1	3′U+905C>G	
ATP2A1*				FBXL19*				C16orf78*	E1	45G>A	K15K
RABEP2*	I3	INV4-56C>T		TMEM142C					I3	INV3+27A>G	
CD19*	E4	1379G>T	P206P	SETD1A*				ZNF423 *			
SPIN1*	E7	6897C>T	S319S	HSD3B7*				C16orf69			
	I7	INV7+278Cdel		STX1B2*				HEATR3 *	I11	INV11-44A>G	
	3′U	3′U+9285C>A[a]		STX4A*	I8	INV8+55C>A		PAPD5*			
LAT	E7	1259G>A	A120A		I8	INV8+65C>T		ADCY7*	E22	24951T>C	Y875Y
BOLA2				ZNF668				BRD7*	I9	INV9-26insT	
GDYD1*				ZNF646*	I1	5′U-108T>G			E16	48481G>A	T570T
SPN*					E2	2722G>C	G907A	NKD1*			
QPRT*				VKORC1*	3′U	3′U+3730G>C[a]		SLIC1*			
C16orf54				BCKDK*				CARD15*			
KIF22*	I12	INV12+70A>G		MYST1*				CYLD*	E17	43909C>T	D805D
MAZ*				PRSS8*	E3	2163C>T	V46V	SALL1*			
PRRT2				PRSS36				FTS*			
MVP*	E10	11504C>T	D525D	FUS*				CAPNS2*			
C16orf53				TRIM72				SLC6A2*			
CDIPT*				PYCARD*				GNAO1*			
PSK-1*				PYDC1*				CNGB1*	E22	51134C>T	N725N
				ITGAM*	I2	INV2+11T>C					

A total of 75 SNPs not reported in the dbSNP database were found in this study

Four SNPs found in 5′-UTR or 3′-UTR happened to be included in the sequenced regions

*Analyzed in seven representative patients: E/I=exon or intron; AA=inferred amino acid change from nonsynonymous SNP; U=UTR

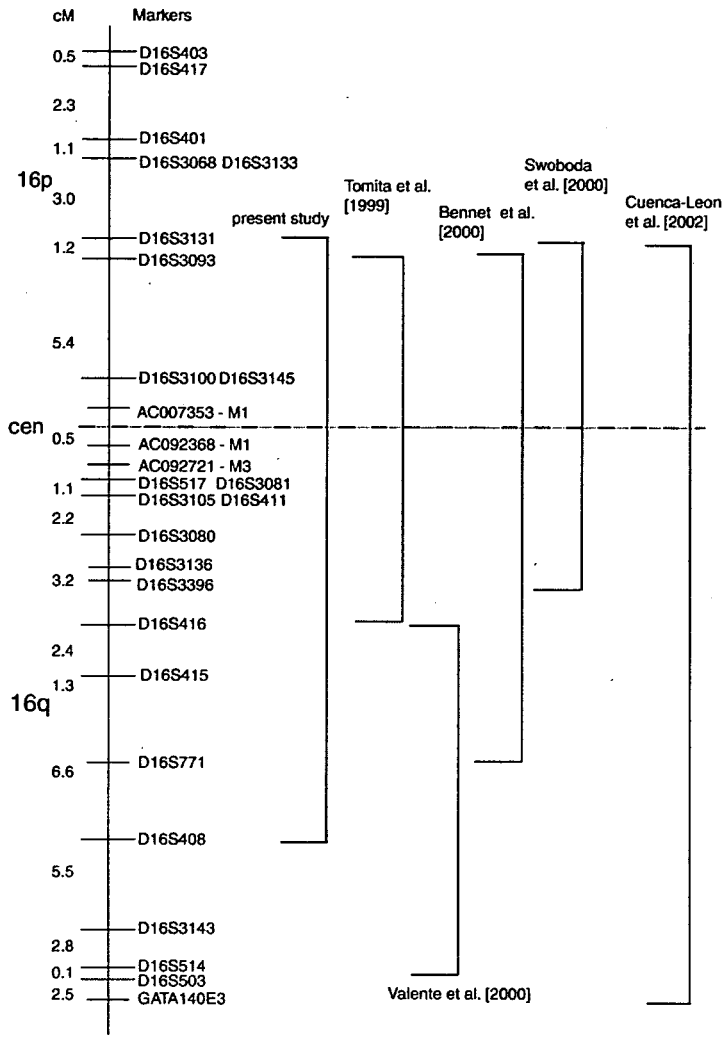

Fig. 4 The PKC-critical region (PKCCR) summarized by five mapping studies (Tomita et al. 1999; Bennett et al. 2000; Swoboda et al. 2000; Cuenca-Leon et al. 2002, present study), as well as a seemingly second PKC locus (EKD2) by Valente et al. (2000). The location of markers and intermarker distances are from the Généthon map (Dib et al. 1996)

Table 3 List of exons that have not been sequenced in the mutation analysis

Gene	Exon
COX6A2	Exon 2, Exon 3
MAZ	Exon 1, Exon 2, Exon 3
VPS35	Exon 9, Exon 10, Exon 11
SULT1A1	Exon 7
SALL1	Exon 2
MGC2474	Exon 2
FLJ43855	Exon 5, Exon 7, Exon 9

Discussion

The PKCCR was assigned to a segment between *D16S3093* and *D16S416* in eight Japanese families (Tomita et al. 1999). It was also mapped between *D16S3100* and *D16S771* in an Afro-Caribbean family (Bennett et al. 2000), between *D16S3131* and *D16S3396* in 11 families of diverse ethnicity (Swoboda et al. 2000), between *D16S3145* and *GATA140E03* in a Spanish family (Cuenca-Leon et al. 2002), and a 24-cM segment between *D16S3131* and *D16S408* in the present study (Fig. 4). Thus, the shortest region of overlap (SRO) did not become narrower than a 12.4-cM segment detected by Tomita et al. (1999). Valente et al. (2000) assigned a form of PKC (a second PKC locus, EKD2), in an Indian family, to a segment between *D16S416* and *D16S503*, the region distinct from those mapped by Tomita et al. (1999) and by Swoboda et al. (2000). Furthermore, two other clinical entities, ICCA and BFIC2, were assigned to a region encompassing the centromere of chromosome 16 (Lee et al. 1998; Hattori et al. 2000; Swoboda et al. 2000; Caraballo et al. 2001; Weber et al. 2004). Since all of these loci were confined to a relatively small region, it is likely that all of these paroxysmal movement dis-

orders actually belong to one disorder and are allelic, as suggested previously (Tomita et al. 1999).

We searched for mutations in almost all protein-coding genes mapped at the PKCCR. In addition, we also analyzed four ion-channel-related genes (*CACNG3*, *SCNN1B*, *SCNN1G*, and *CNGB1*), albeit located outside the PKCCR, since many episodic neurologic disorders, such as muscle diseases, epilepsy, and movement disorders, are known as ion-channel abnormalities (Bhatia et al. 2000). However, 14 coding exons in seven genes (Table 3) were not analyzed because of difficulties in PCR-amplification.

In the present study on a total of 157 genes, we failed to identify any causative mutations that can explain PKC in all of the seven families examined. However, two nonsynonymous substitutions, 6186C>A in exon 3 of *SCNN1G* and 45842A>G in exon 29 of *ITGAL*, which were co-segregated with PKC in Families C and F, respectively, which were not found in normal control individuals, might be implicated in PKC. In other words, they were not able to be totally ruled out from the candidacy for PKC. It thus remains to be investigated whether another mutation in either gene is found in other PKC families.

Although the mapping of PKC was successful in at least nine studies, causative mutations have been uncovered. This may imply that PKC is caused by aberrations other than exonic mutations, such as a deletion or insertion, in the promoter regions, including the 5′-UTR or 3′-UTR. However, there is still a possibility for usual exonic mutations in a novel gene not annotated in public databases. As PKC itself is, generally, a viable disorder with which patients may show high reproductive fitness, such a mutated allele may be transmitted through many generations. A chromosomal rearrangement is another possibility. The pericentromeric region of chromosome 16 has a large heterochromatin (C-band) block that contains several duplicated regions, through which, frequent chromosomal rearrangements occur (Loftus et al. 1999). It remains also to be seen whether PKC patients within a family share such a variant.

Acknowledgments We are indebted to the family members for their participation in this research. We especially thank Ms. Y. Noguchi and A. Goto for their technical assistance. N.N. was supported in part by a Grant-in-Aid for Scientific Research (Category S, grant no. 13854024; Priority Areas for Applied Genomics, grant no. 17019055) from the Ministry of Education, Culture, Sports, Science and Technology (MEXT) of Japan, and by Solution Oriented Research of Science and Technology (SORST) from the Japan Science and Technology Agency (JST). K.Y. was supported by a Grant-in-Aid for Scientific Research for Priority Areas (grant no. 17590288) from the MEXT of Japan.

References

Bennett LB, Roach ES, Bowcock AM (2000) A locus for paroxysmal kinesigenic dyskinesia maps to human chromosome 16. Neurology 54(1):125–130

Bhatia KP (1999) The paroxysmal dyskinesias. J Neurol 246(3):149–155

Bhatia KP, Griggs RC, Ptáček LJ (2000) Episodic movement disorders as channelopathies. Mov Disord 15(3):429–433

Caraballo R, Pavek S, Lemainque A, Gastaldi G, Echenne B, Motte J, Genton P, Cersósimo R, Humbertclaude V, Fejerman N, Monaco AP, Lathrop MG, Rochette J, Szepetowski P (2001) Linkage of benign familial infantile convulsions to chromosome 16p12-q12 suggests allelism to the infantile convulsions and choreoathetosis syndrome. Am J Hum Genet 68(3):788–794

Cuenca-Leon E, Cormand B, Thomson T, Macaya A (2002) Paroxysmal kinesigenic dyskinesia and generalized seizures: clinical and genetic analysis in a Spanish pedigree. Neuropediat 33(6):288–293

Dib C, Faure S, Fizames C, Samson D, Drouot N, Vignal A, Millasseau P, Marc S, Hazan J, Seboun E, Lathrop M, Gyapay G, Morissette J, Weissenbach J (1996) A comprehensive genetic map of the human genome based on 5246 microsatellites. Nature 380:152–154

Hattori H, Fujii T, Nigami H, Higuchi Y, Tsuji M, Hamada Y (2000) Co-segregation of benign infantile convulsions and paroxysmal kinesigenic choreoathetosis. Brain Develop 22(7):432–435

Kato N, Sadamatsu M, Kikuchi T, Niikawa N, Fukuyama Y (2006) Paroxysmal kinesigenic choreoathetosis: from first discovery in 1892 to genetic linkage with benign familial infantile convulsions. Epilepsy Res 70(Suppl 1):174–184

Lee W-L, Tay A, Ong H-T, Goh L-M, Monaco AP, Szepetowski P (1998) Association of infantile convulsions with paroxysmal dyskinesias (ICCA syndrome): confirmation of linkage to human chromosome 16p12-q12 in a Chinese family. Hum Genet 103(5):608–612

Loftus BJ, Kim UJ, Sneddon VP, Kalush F, Brandon R, Fuhrmann J, Mason T, Crosby ML, Barnstead M, Cronin L, Deslattes Mays A, Cao Y, Xu RX, Kang HL, Mitchell S, Eichler EE, Harris PC, Venter JC, Adams MD (1999) Genome duplications and other features in 12 Mb of DNA sequence from human chromosome 16p and 16q. Genomics 60(3):295–308

Nagamitsu S, Matsuishi T, Hashimoto K, Yamashita Y, Aihara M, Shimizu K, Mizuguchi M, Iwamoto H, Saitoh S, Hirano Y, Kato H, Fukuyama Y, Simada M (1999) Multicenter study of paroxysmal dyskinesias in Japan—clinical and pedigree analysis. Mov Disord 14(4):658–663

Sadamatsu M, Masui A, Sakai T, Kunugi H, Nanko S, Kato N (1999) Familial paroxysmal kinesigenic choreoathetosis: an electrophysiologic and genotypic analysis. Epilepsia 40(7):942–949

Swoboda KJ, Soong B, McKenna C, Brunt ER, Litt M, Bale JF Jr, Ashizawa T, Bennett LB, Bowcock AM, Roach ES, Gerson D, Matsuura T, Heydemann PT, Nespeca MP, Jankovic J, Leppert M, Ptáček LJ (2000) Paroxysmal kinesigenic dyskinesia and infantile convulsions: clinical and linkage studies. Neurology 55(2):224–230

Tomita H, Nagamitsu S, Wakui K, Fukushima Y, Yamada K, Sadamitsu M, Masui A, Konishi T, Matsuishi T, Aihara M, Shimizu K, Hashimoto K, Mineta M, Matsushima M, Tsujita T, Saito M, Tanaka H, Tsuji S, Takagi T, Nakamura Y, Nakano S, Kato N, Nakane Y, Niikawa N (1999) Paroxys-